Photodegradation mechanisms and kinetics of Eosin-Y in oxic and anoxic conditions

Photodegradation mechanisms and kinetics of Eosin-Y in oxic and anoxic conditions

Alba Alvarez-Martin[a,*], Stanislav Trashin[a], Matthias Cuykx[b], Adrian Covaci[b], Karolien De Wael[a], Koen Janssens[a]

[a] AXES, Department of Chemistry, University of Antwerp, Groenenborgerlaan 171, 2020 Antwerp, Belgium

[b] Toxicological Center, University of Antwerp, Universiteitsplein 1, 2610 Wilrijk, Belgium

*Corresponding author E-mail address: alba.alvarez@usal.es (Alba Alvarez-Martin)

Keywords: Eosin, Red Dye, Photodegradation, Anoxic conditions, LC-QTOFMS, Electrochemistry

Abstract

Lakes based on Eosin-Y are extensively used by 19th century artists. Unfortunately, the identification of these pigments in paintings is a difficult task because Eosin-Y degrades very fast under the influence of light.

The characterization of the (photo)degradation products of Eosin-Y can be very useful for the identification of these pigments in historic works of art and related cultural heritage artifacts. Furthermore, knowledge on how different factors influence the discoloration process (e.g. different types of irradiation sources and presence/absence of oxygen) is a valuable tool for preventive conservation.

To this aim we performed a study on the photodegradation of Eosin-Y in solution under different illumination and in both oxic and anoxic conditions. The photodegradation of Eosin-Y was monitored by UV-VIS spectrophotometry, LC-QTOFMS and electrochemistry techniques.

Results indicated higher degradation rates, by a factor of 20 or higher, under illumination with wavelengths near to the main absorbance band of the red pigment. Two different degradation pathways are observed under the conditions studied. LC-QTOFMS and electrochemistry suggested that in the presence of oxygen the degradation mechanism is an oxidative process where the breakdown of the structure causes the total discoloration. Meanwhile under anoxic conditions, a debromination process takes place while the chromophore, and consequently the color of the molecule in solution, remains essentially intact.

1. Introduction

Eosin-Y is a xanthene red dye (Acid Red 87, CI 45380) defined by a conjugated π system, resulting in a strong absorption in the visible range of the spectrum, giving rise to the characteristic red color. The molecular structures of this compound are shown in Fig. 1.

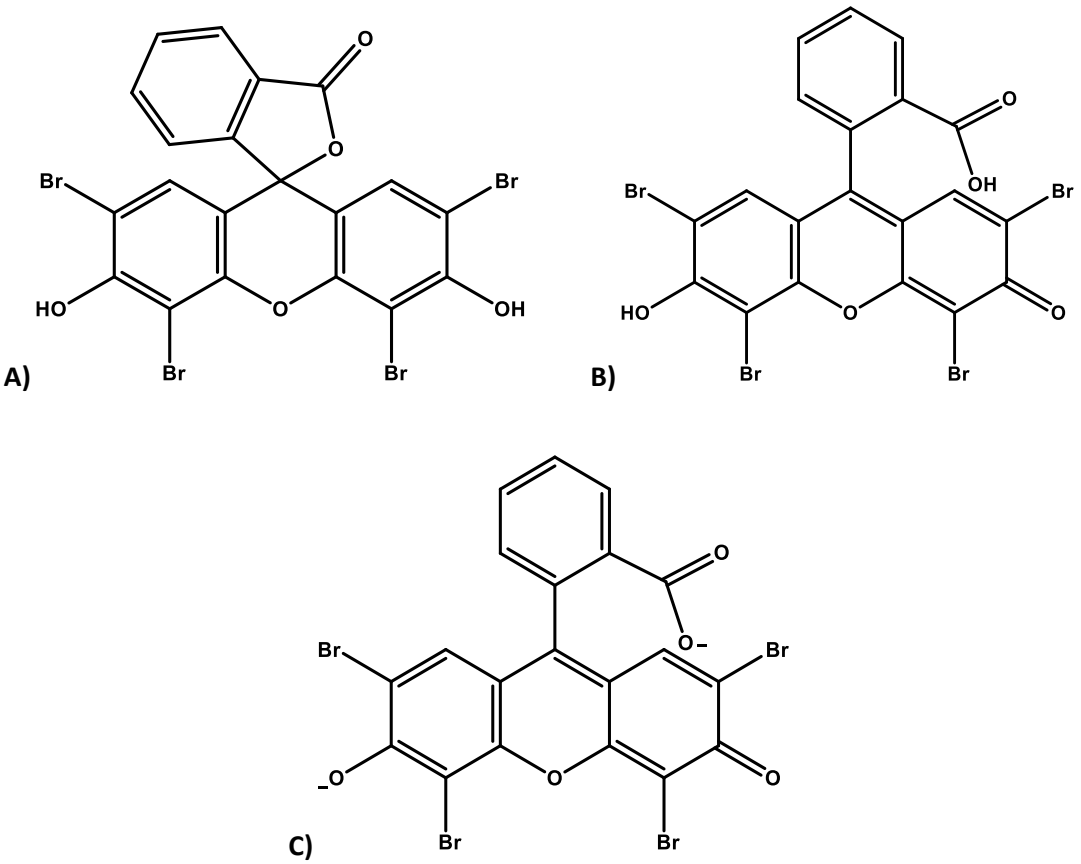

Fig. 1. Chemical structures of Eosin-Y. Lactone form (A), Quinoid form (B) and Dianionic form (C).

Eosin was discovered in 1873 by Henry Caro [1] by bromination of fluorescein and commercialized as a textile dye in the same year; from that moment in time, it has been extensively used in the manufacturing and textile industry.

Eosin was commercialized as an artistic dye from 1880 onwards. The soluble dye Eosin-Y can be converted into an insoluble pigment named *geranium lake* by precipitation with aluminum, lead or potassium salts. These xanthene lakes are composed of a metal ion complexed by two Eosin molecules with a similar coordination to anthraquinone dyes [2]. A recent study has reported that the carboxylic group coordinates the metal in Eosin-based lakes [3]. Geranium lake was used by 19^{th} century artists such as Vincent Van Gogh (1853-1890) or Paul Gauguin (1848-1903) due to its wide variety of possible hues; depending upon the metal used in the precipitation, this hue can range from orange-scarlet to bluish-red [1]. Both artists started to notice the discoloration in some of their paintings already a few months after finishing; Eosin has a marked tendency to fade upon exposure to light [4, 5]. The identification of Eosin-Y and the characterization of its degradation products in paintings represents a challenge because of (i) the low concentration/amount remaining intact after several years/decades of aging, (ii) the difficulty in obtaining samples for analysis, and (iii) differences in (degradation) behavior when Eosin is combined with organic or inorganic pigments, binding media or varnish [1,4].

Likewise, light can cause lakes used in cultural objects to lose their color, it can also accelerate the discoloration of the Eosin-Y in solution. Although the photodegradation of organic pigments (also) depends on the paint medium and the environmental condition, several studies have demonstrated that solution phase systems may serve as simple models to estimate the kinetic behavior and discoloration mechanism of pigments in solid form [6,7]. Monitoring the (photo)degradation process of Eosin-Y is challenging because this dye is extremely light sensitive and features a strong pH dependence [8,9].

Another factor influencing the degradation kinetics of organic dyes is the amount of oxygen present in the environment. Anoxic storage conditions have been extensively investigated as a preservation method for historical artifacts [10,11]. Although most of the studies have revealed that anoxia

would be expected to slow the degradation process, it is remarkable that some organic dyes exhibit a more pronounced degradation in a reduced oxygen atmosphere [12,13]. There are only a few reports about the influence of oxygen on the degradation mechanism or the stability of organic dyes stored under nitrogen atmosphere [14].

The interaction between oxygen and organic dyes has been recently studied in the field of organocatalysis. In the last decade, new strategies have been suggested to increase the yield of organocatalytic reactions; one of these involves the combination of an organocatalytic cycle with a photocatalysis strategy [15]. A group of red dyes, included Eosin-Y, has been proposed as catalysts in a metal-free photoredox catalysis as a substitute for more typical organometallic compounds (such as ruthenium or iridium salts) [16,17]: where the excitation of the dye by green light is followed by an electron transfer from the excited triplet state of the molecule [18]. One can consider the analogy between photoredox catalysis and the photo-degradation of Eosin-Y in solution as the starting point for proposing a mechanism for the light-induced aging of Eosin-Y in cultural artifacts.

In this work, the influence of the wavelength of light and the influence of oxygen on the discoloration process of Eosin-Y were studied. Three different sources of light were employed to observe significant changes in the UV-VIS absorbance spectrum of Eosin-Y over the course of an irradiation experiment. Both oxic and anoxic conditions were investigated. By monitoring the changes in the absorption spectra after irradiating the solution under different conditions, information on the nature of the degradation process is obtained. In addition, chromatographic studies were undertaken to identify secondary products. Recently, amperometry and voltammetry have been proposed as alternative means of studying the photodegradation process of inorganic pigments [19,20]. These electrochemical methods allowed to monitor the photodegradation of

pigments in-situ and to clarify their photodegradation mechanism and kinetics under different environmental conditions.

The characterization of the behavior of Eosin-Y in solution under different conditions can provide relevant information on the kinetics and molecular mechanism of photodegradation; these insights can be used to improve the long-term storage conditions of cultural artifacts in which Eosin-Y was used.

2. Materials and methods

2.1. Sample preparation

Commercial Eosin-Y (99% Sigma-Aldrich) was used without further purification. A stock solution of 3.1 mM was stored in the dark and used for preparation of a dilute working solution (15 µM). The pH of the working solution was 10, at which Eosin-Y is exclusively present in its dianionic form [21]. The study of this form is relevant since to the manufacture of geranium lake is carried out in alkaline pH (8-12) conditions [22].

2.2. Photodegradation experiments

A sealable quartz cuvette (Hellma® Analytics, 117-100-10-40) containing the stock solution was irradiated with three different sources of light: under broad band UV light (UVA and UVB: 280 to 400 nm) in a solar irradiation chamber and by means of two types of laser: 405 nm (blue) and 532 nm (green). The photon flux in the solar chamber and emitted by the blue and green lasers were 1.7-1.5, 2.0 and 2.7 x 10^{18} photon m^{-2} s^{-1}, respectively.

In order to create anoxic conditions, the cuvette was sealed with a screw cap containing a rubber seal; two needles served as inlet and outlet. Dry nitrogen was bubbled through the sealed cuvette containing 3 mL of solution for 1 hour prior to light exposure.

2.3. UV-VIS absorbance spectrophotometry

The degradation of eosin in the stock solution was monitored as a function of exposure time by recording absorbance spectra on a Perkin Elmer Lambda 750 in the 800-200 nm range with 266.75 nm/min scan speed; each absorption spectrum took a recording time of 2.24 min. The UV-VIS beam intensity employed for the measurements was such that we can assume no additional degradation took place during/as a result of the UV-VIS measurements itself. The UV Win Lab (Version 6.2.0, Perkin Elmer) software was used for data processing and viewing.

2.4. Degradation kinetic studies

Absorbance spectra were recorded before and after exposure of the solution to light for different lengths of time. The degradation was monitored up to 150 min, 36 h and 62 h for the samples irradiated with green, blue and UV light, respectively. The progressive decline of the main band intensity (517 nm) of Eosin-Y was used as a reference to evaluate the degradation kinetics. With the aim of determining the rate constants and kinetic order of the degradation, linear regression of the integrated absorption peak intensity data was carried out.

2.5. Chromatographic study of the Eosin-Y degradation products

The aqueous samples were centrifuged through a 0.22 µm nylon filter and stored in brown vials for injection. The illumination in the auto-sampler was switched off and the temperature was kept at 4 °C to prevent degradation prior to analysis. The samples were injected on a Kinetex® C18 column (150 x 2.1 mm, 1.7 µm particle size; Phenomenex, the Netherlands) using an Agilent 1290 chromatographic system (Agilent, Santa Clara, USA); the injection volume was 1 µL. The mobile phases were A) ultra-pure Milli-Q water (Elgo Lab, Tienen, Belgium) with 0.1 % (v/v) of formic

156 acid and B) Methanol/ultra-pure Milli-Q water (90/10, v/v) with 0.1 % (v/v) of formic acid. The
157 separation was performed using a gradient elution starting at 5 % of mobile phase B for 1 min,
158 increasing to 100 % B at 10 min. The column was rinsed for 1 min and re-equilibrated for 3 min to
159 prepare the column for the next analysis. The flow rate was kept constant at 0.4 mL/min at a
160 temperature of 45 °C. The eluting compounds were nebulized with the Agilent Jet Stream-nebulizer
161 and detected using an Agilent 6530 quadrupole-time of flight (QTOF, Agilent). The drying gas
162 temperature was 300 °C, the gas flow was 8 L/min. The sheath gas temperature and flow were 350
163 °C and 11 L/min, respectively. The nebulizer pressure was 30 psi.
164 The analysis was performed in both negative and positive ionization modes. For both modes, the
165 capillary voltage, nozzle voltage and fragmentor voltage were 4000 V, 1000 V and 150 V,
166 respectively. The QTOF was equilibrated using a mix of reference masses. Continuous
167 recalibration was performed on the injected compounds (trifluoroacetic acid, purine and HP-921,
168 giving a reference m/z of 121.0508 and 922.0098 in positive mode and 112.9855 and 966.0007 in
169 negative mode, respectively). MS scans were acquired at 2 scans per second.
170 The data were analyzed using Mass-Hunter (Agilent, v. B.06.00) and Mass-Profiler Professional
171 (Agilent, v. 12.5). Degradation products of Eosin-Y were searched for using an untargeted
172 approach: molecular features were extracted with the Molecular Feature Extractor algorithm (MFE,
173 Agilent) using the following parameters: unbiased extraction with spacing tolerance of 15 ppm and
174 a symmetric mass defect of -0.2895 to +0.05 to increase the selectivity for brominated compounds.
175 Ion adducts searched were proton and sodium adducts in positive mode, in negative mode only the
176 loss of a proton was considered. The score threshold was put at >40 to reduce false negative
177 compounds; filtering of false positive compounds was performed with Mass-Profiler Professional.
178 Identical molecular features between samples were aligned with a retention window of 0.2 min and
179 a mass difference tolerance of 20 ppm. The obtained matrix was then searched for molecular

features which had trends that relate to chemical degradation, i.e. if their signal showed an increasing (formation), decreasing (degradation) or complex (formation and degradation combined) trend. The signals were identified in the Mass-Hunter software using the Molecular Formula Generator algorithm (MFG, Agilent). The results were manually checked for mass accuracy, isotope pattern, and isotope spacing to confirm the identification.

2.6. Electrochemistry

Electrochemical measurements were done in a three-electrode cell using a saturated Calomel reference electrode (potential of 0.248 V versus SHE), a glassy carbon rod as a counter electrode, and a screen-printed carbon electrode type IS-C (ItalSens, Florence, Italy) as a disposable working electrode. The cell was connected to a potentiostat model μAutolab III (Metrohm-Autolab BV, the Netherlands) controlled by a computer. Phosphate buffer at pH 7, supported with 0.1 M KCl, was used as a background electrolyte. Photocurrents were measured as a difference between the current under illumination and the background current before illumination.

3. Results and discussion

3.1. UV-VIS spectra and degradation kinetics under oxic conditions

3.1.1. Absorbance spectra

As shown in Fig. 2, the UV-VIS absorbance spectra of Eosin-Y feature a major band at 517 nm, assigned to the chromophore responsible for its red color. The shoulder at 490 nm in the initial spectrum has been ascribed to the dimeric form of Eosin-Y [23]. The spectra also show three other well-defined, but less intense bands at 341, 301 and 255 nm assigned to $\pi \rightarrow \pi^*$ transitions in the aromatic rings. The molar absorptivity coefficients (ε) of the absorption bands are reported in the

204 literature [24] and match with the experimental values calculated in the present work (data shown
205 in Supplementary Information, Table SI.1).
206 Under oxic conditions, during irradiation with the three light sources an identical spectral change
207 can be observed: the main absorbance band centered at 517 nm decays over time, causing the
208 initially red solution to lose its color. In accordance with the ε-values of Eosin-Y at 405 and 532
209 nm (see Table SI.1), the efficiency of degradation with the green laser is significantly higher than
210 with the blue laser: while ca. 12 h of irradiation using blue light was required to reduce the main
211 peak intensity to half of its original value, only ca. 30 min were required with the green laser. In
212 addition, only with green laser irradiation, a rise in absorbance in the 360-440 nm range was
213 observed.

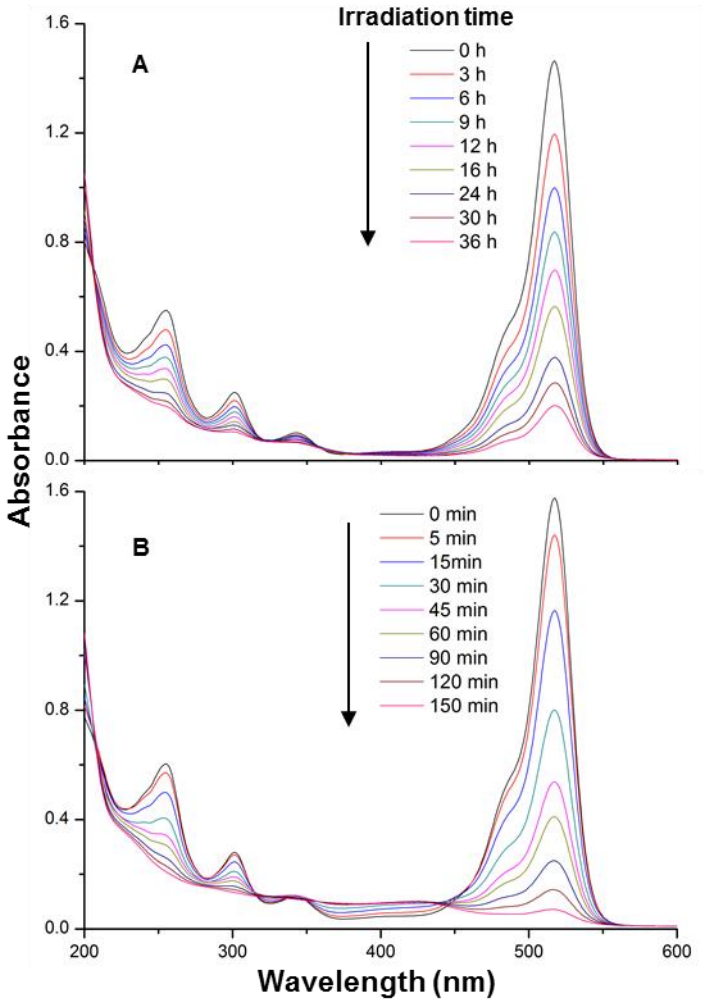

Fig. 2. UV-VIS spectra of photodegradation of Eosin-Y under oxic conditions irradiated with (A) the 405 nm (blue) and (B) the 532 nm (green) laser.

The solution sample irradiated with the blue laser (Fig. 2A and Fig. SI.1) shows three isosbestic points at 380, 360 and 320 nm during the first 16 hours of irradiation. The sample irradiated with the green laser (Fig. 2B and Fig. SI.1.) also shows three isosbestic points (around 450, 340 and 315 nm) during the first hour of irradiation. The presence of these isosbestic points and the change in the absorbance spectrum are indicative of a relatively simple degradation, in which the original red colored form of the dye is converted into an uncolored form that no longer shows an important

absorption peak in the visual range. After 150 min of green laser irradiation, at 517 nm, a residual absorbance of ca. 10% of the original value is observed.

3.1.2. Kinetics

The 517 nm absorbance peak integral versus time curve was fitted based upon integer-order kinetics. The degradation curve fits to the first order better than the zero or second order. In order to compare the degradation rate under different excitation conditions, the linear relationship between $\ln[A_{517\ nm}(t = 0)/A_{517\ nm}(t)]$ versus irradiation time t is plotted in Fig. 3. The slopes of the linear regression curves show the more rapid degradation of Eosin-Y under green laser irradiation; the rate constants are reported in Table 1. The value of the rate constant for green light irradiation is the highest since the green laser (532 nm) closely matches the intense absorbance band of eosin at 517 nm, in contrast to the blue laser that emits at 405 nm and the lamps in the solar chamber that irradiate from 300 to 350 nm.

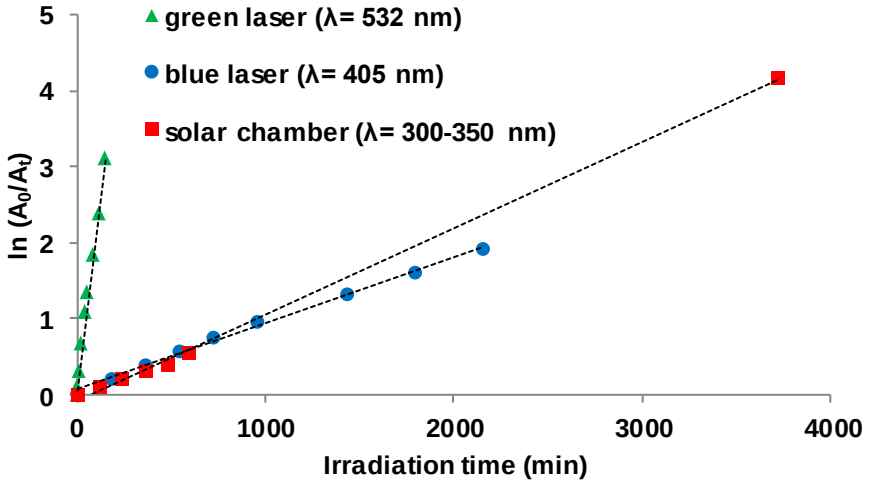

Fig. 3. First-order linear plot of $\ln[A_{517nm}(t=0)/A_{517nm}(t)]$vs the irradiation time t under irradiation by three light sources (532 nm, 405 nm and 300-350 nm).

A first order kinetic behavior has been described for other red pigments, such as the alizarine lake [25]. The mechanism of degradation of similar organic red dyes is attributed to a structural change in the chromophore due to the irradiation, for example ring opening or bond breaking, leading to a change of the hydrogen bonds in the structure [7].

Light source (nm)	Photon flux (10^{18}) (photon m^{-2} s^{-1})	Oxic/ Rate constant (1^{st} order) (min^{-1})	Anoxic/ Rate constant (pseudo 1^{st} order) (min^{-1})
Solar chamber (300-350)	2.5-2.9	$k_1 = 0.0011$	-
Blue laser (405)	3.38	$k_1 = 0.0009$	-
Green laser (532)	4.4	$k_1 = 0.0207$	$k_1 = 0.0378$ $k_2 = 0.019$

Table 1. Rate constants for degradation kinetics of eosin in solution under oxic and anoxic conditions.

3.2. UV-VIS spectra and degradation kinetics under anoxic conditions

When the oxygen in the solution is removed via N_2 bubbling, a significant modification in the absorption spectra can be observed (see Fig. 4 and Fig. SI.2). Under these anoxic conditions, already after ca. 15 min of green laser irradiation, the main band intensity has fallen to half of its original value. The 517 nm absorbance band first decreases rapidly and then exhibits a slower decrease. After 45 min of irradiation, the main peak at 517 nm and the shoulder at 493 nm have almost merged into a single broad peak. At 340 and 315 nm the same isosbestic points as in oxic conditions are observed. However, the isosbestic point centered at 450 nm is now at 465 nm. Additional isosbestic points are detected at 290, 265 and 230 nm but only during the first 30 min

of irradiation. The change in speed of color loss and the loss of the isosbestic points in the 230-290 nm range suggest that multiple transformations are involved in the degradation process [26].

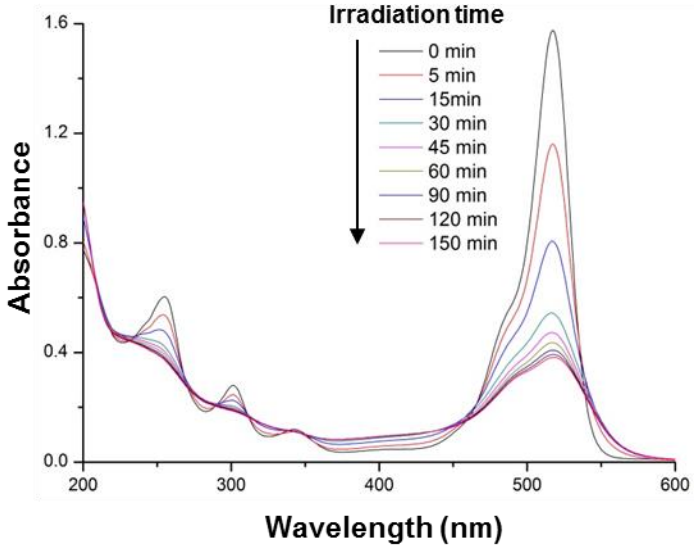

Fig. 4. UV-VIS spectra of Eosin-Y during photodegradation under anoxic conditions, irradiated with a 532 nm laser.

By comparing the initial and final absorbance (after 150 min of irradiation) at 517 nm under anoxia, a residual absorbance band was found; this may suggest the formation of a degradation product that absorbs in the same spectral region, possibly with a similar structure as that of Eosin-Y, but with a lower extinction coefficient. Such a product could also explain the rise of the baseline in the range 465-340 nm with irradiation time. The presence of new degradation product(s) might explain the overlap in the absorbance spectra due to new bands observed at 250 and 490 nm. The main peak in the final spectra could be described as a sum of two bands at 490 nm and 517 nm. From the comparison of the spectra in Fig. 2 and 4, it follows that the dimerization (shoulder at 490 nm)

is more favorable under anoxic conditions due to an increase in abundance of the monomeric reactive species.

The evidence of the discoloration in solution could be clearly observed visually: under oxic conditions, the solution turned pale pink-yellow and the solution was colorless at the end of the degradation the solution. The excited eosin molecules may have reacted among each other or with other nearby molecules (such as water or oxygen), enhancing the degradation process. However, in anoxic conditions, the solution remained red, indicating that in the presence of N_2, Eosin-Y does not directly transform into a colorless form. Instead, an intermediate (colored) form was generated that altered the red hue of the solution, rendering the absorption of green laser light less effective since the dimer form is the main form present in the solution. In Fig. SI.3, photographs are provided of the gradually discoloration of the solutions under green laser irradiation. After 150 min of irradiation, at 517 nm, a residual absorbance of ca 25% of the original value is observed.

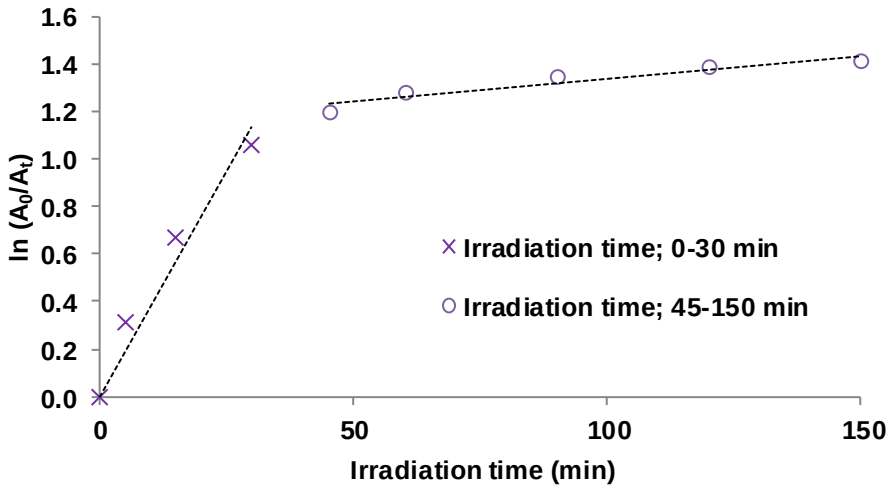

Fig. 5. Pseudo first-order linear plot of $\ln[(A_{517nm}(t = 0)/A_{517nm}(t)]$ vs irradiation time *t* under 532 nm (green) laser irradiation and anoxic conditions.

The rate constants of the transformation under anoxic conditions were again obtained by monitoring the absorbance at 517 nm. As shown in Fig. 5, the log of the normalized absorbance appears to decrease (quasi-)linearly with irradiation time up to 30 min; after this point, another, slower, linear decrease is observed. Consistent with the observance of the isosbestic points, Fig. 5 clearly suggest that two sequential chemical transformations are taking place. In Table 1, the rate constants of both domains are listed.

Eosin-Y therefore appears to degrade via a mechanism similar to that proposed by Feller for the degradation of organic dyes involving two first-order kinetic transformations [27].

3.3. Chromatographic analysis

LC-MS analyses of the partially photodegraded Eosin-Y solutions were performed to ascribe the differences in the photodegradation processes under distinct environment conditions and identify possible degradation products. Solutions irradiated with both the blue and green lasers in oxic conditions were analyzed; additional experiments involved solutions exposed to green light in anoxic conditions.

The LC-MS data confirmed the degradation trends obtained by means of UV-VIS spectroscopy: irradiation with a green laser increased the degradation speed (Fig. SI.4). Anoxic conditions degraded the parent compound more efficiently than oxic conditions. However, the Eosin-Y already appeared fully degraded after one hour of exposure to green laser light under anoxic conditions. The UV-VIS data, on the other hand showed a rest-absorbance even 150 min after exposure to light. A possible explanation for this discrepancy are the absorbance properties of the degradation products: although Eosin-Y itself was not present after one hour of irradiation, other chromophores, still able to absorb light, remain, resulting in the background absorption.

In all analyzed solutions, only one debrominated product ($C_{20}H_9O_5Br_3$, m/z = 567.79) was identified. The foregoing tribrominated product is formed during the first minutes of the irradiation experiment and further degrades over time (Fig. 6A). Green laser irradiation under anoxic conditions gave rise to a higher maximum abundance of this product than the other conditions. Under oxic conditions, the debromination compounds appeared to be more stable while anoxia caused it to break down faster.

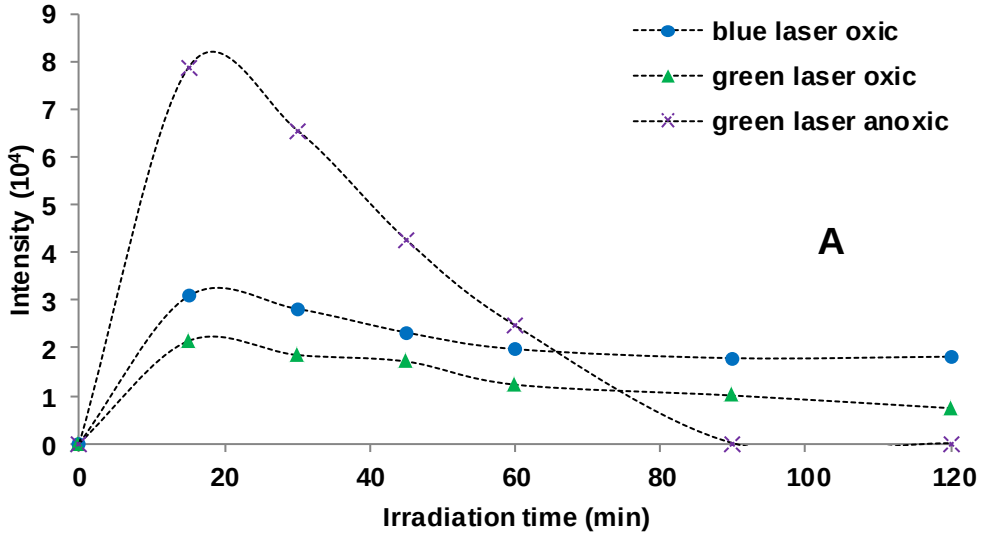

321

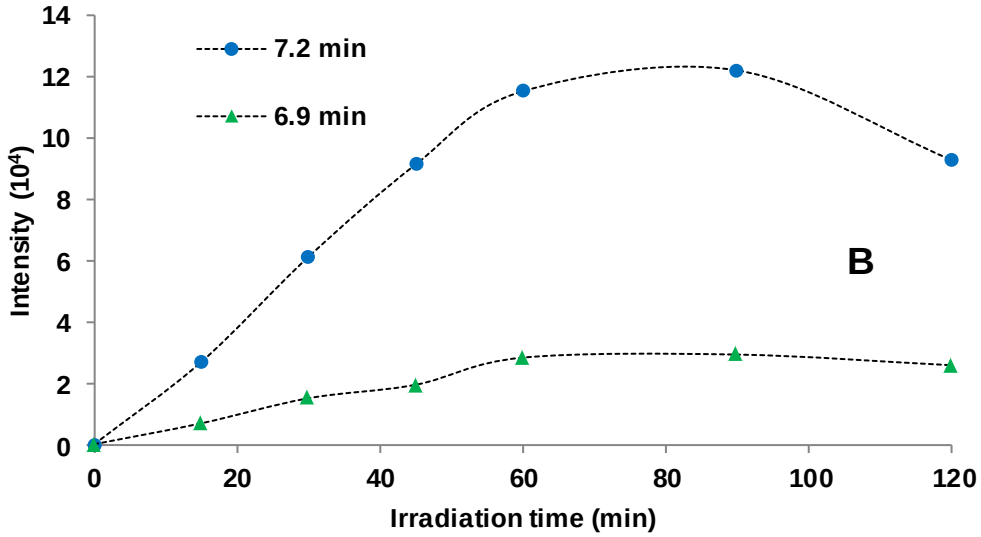

322

323 **Fig. 6.** Formation and decay of transformation products (A) $C_{20}H_9O_5Br_3$ (m/z = 566.7886) and

324 (B) $C_{20}H_{10}O_5Br_2$ (m/z = 488.8759).

325

326 Only in the solutions exposed to the green laser under anoxic conditions, two other degradation

327 products having formula $C_{20}H_{10}O_5Br_2$ (m/z = 488.8759) were found (Fig. 6B); the onset of their

328 formation coincides with the decay of $C_{20}H_9O_5Br_3$. This suggests that the initial debromination is

followed by a second step, resulting in two of the four Br atoms per Eosin-Y molecule being replaced by H-atoms. Two chromatographic peaks at 6.9 and 7.2 min retention time were observed in positive mode; we associate them to two different debromination products that only differing in the position of remaining Br atoms. In negative mode however, only the peak at 7.2 min was observed. This could be explained by either lower ionization efficiency or by slower kinetics, leading to the formation of less transformation product. The abundance of both $C_{20}H_{11}O_5Br_2$ signals shows an increase in the first hour of irradiation, followed by a plateau/slow decrease later in the experiment. The formation of the two debrominated transformation products is significantly faster than their decay and of the same speed as the decay of $C_{20}H_9O_5Br_3$. The apex of the $C_{20}H_{10}O_5Br_2$ abundance curve is situated at 60-80 min after the start of the irradiation, i.e., 40-60 min later than that of the single debromination compound, that peaks 20 min after the start if irradiation. The slow decrease observed after the maximum can be attributed to both the exhaustion of the parent $C_{20}H_9O_5Br_3$ and the further degradation of $C_{20}H_{10}O_5Br_2$. These observations are qualitatively consistent with the UV-VIS data of Fig. 5.

The above observations are consistent with the available literature and with the spectroscopic observations above. The debromination process has been suggested as the result of photodegradation of Eosin-Y in alkaline solutions; independent of the degree of (de)bromination, the UV-VIS spectra of the debrominated species are qualitatively identical [28]. The partially debrominated Eosin-Y species have been associated with an increased absorbance around 400 nm [29]. As it can be seen in Fig. 2 and 5, such increase is indeed observable in the range 350-450 nm under green laser irradiation in oxic and anoxic conditions. Some authors have suggested the generation of di-bromofluorescein ($C_{20}H_{10}O_5Br_2$) and fluorescein ($C_{20}H_{12}O_5$) as intermediate and final debromination product of Eosin-Y; these compounds have their main absorbance bands at 512 and 496 nm, respectively [29,30]. The shift of the main UV-VIS absorbance band of Eosin-Y

to lower wavelengths that is visible in Fig. 5 may therefore be interpreted as a sign of the presence of these species under anoxic conditions.

The results suggest that in oxic conditions, oxygen radicals may attack the conjugated systems of the Eosin-Y, causing its breakdown and resulting in a complete loss of the color. On the other hand, under anoxic conditions, a (two step) debromination mechanism improves the oxidative stability [31,32]. Since both $C_{20}H_9O_5Br_3$ and $C_{20}H_{10}O_5Br_2$ still contain chromophoric groups similar to those of the original Eosin-Y, this mechanism is consistent with a lower degree of discoloration at the end of the irradiation experiments in anoxic relative to oxic conditions., the following simplified degradation mechanisms can be proposed, consistent with the results obtained by spectroscopic and chromatographic analyses:

$$Oxic\ conditions: Eosin\ Y \overset{k_1}{\rightarrow} Eosin\ Y\ (-Br) \rightarrow\rightarrow \text{chromophore breakdown}$$

$$Anoxic\ conditions: Eosin\ Y \overset{k_1}{\rightarrow} Eosin\ Y\ (-Br) \overset{k_2}{\rightarrow} Eosin\ Y\ (-2Br) \rightarrow\rightarrow \text{Fluorescein}$$

3.4. Electrochemical experiments

3.4.1. Mechanism of degradation

From the experiments described above, it is clear that the degradation mechanism of Eosin-Y differs in the presence and absence of oxygen. To explain this difference, we put forward the hypothesis that the observed differences in degradation kinetics are related to the effective average lifetime of the excited state of Eosin-Y. Under green light illumination, the photo-excited high energy state of Eosin-Y generally may evolve into a comparatively long-lived high energy triplet state (with a life time of 24 μs [33]). In the absence of oxygen (under N_2 atmosphere), some of the excited Eosin-Y molecules (EY* in Fig. 7) may (eventually) degrade through debromination (Fig. 7, scheme A). In the presence of oxygen, on the other hand, the EY* can be rapidly quenched by

the triplet state of oxygen (Fig. 7, scheme B). This process results in the formation of highly reactive singlet oxygen ($^1O_2$) and related secondary oxygen species (the latter are formed in reactions of singlet oxygen with organic molecules). This is consistent with literature reports on the high quantum yield of singlet oxygen photogeneration by Eosin-Y [34-36]. The short life-time of singlet oxygen can be responsible for apparently slower degradation kinetics of Eosin-Y in oxic conditions compared to anoxic conditions, although oxygen results in complete discoloration because of more destructive chemical reactions.

3.4.2. UV-vis and electrochemical measurements in the presence of hydroquinone.

In order to test the above hypothesis, an experiment involving a singlet oxygen quencher was performed. If the hypothesis is valid, the presence of quenchers should improve the stability of Eosin-Y in oxic conditions. Hydroquinone (HQ) quickly oxidizes into benzoquinone (BQ) by $^1O_2$ and can thus act as $^1O_2$ quencher [37]. Advantageously, the redox transformation of HQ can be readily monitored *in-situ* by electrochemical means. In order to avoid autoxidation of HQ at increased pH values, measurements with HQ were conducted in a phosphate buffer at pH 7; the results are shown in Table 2 and Fig. SI.5-SI.7. Consistent with the literature [21,24], the absorption spectra and the ionic form of Eosin-Y do not change above pH 7. Introduction of an excess of HQ into the solution (i.e., 10 times the concentration of Eosin-Y) significantly suppressed the photodegradation of Eosin-Y in oxic conditions (Table 3, Fig. 7: mechanism C and Fig. 8), while simultaneously, the formation of BQ was observed with UV-VIS (intense absorption peak at 248 nm).

Conditions	Average current ± SD (n=4), nA	
	No Eosin-Y	10 μM Eosin-Y
Air saturated buffer without HQ	-1.5±0.09	-1.7±0.14
10 μM HQ in air saturated buffer	-2.1±0.04	-121.8±5.5
10 μM HQ in N_2 saturated buffer	-	<0.1

Table 2.Current increase under illumination of Eosin-Y and HQ solutions.

	% Degradation [a]	
	60 min	120 min
15 μM Eosin-Y, pH 12	74	91
15 μM Eosin-Y, pH 7	69	92
15 μM Eosin-Y + 150 μM HQ, pH 7	27	47
15 μM Eosin-Y + 450 μM HQ, pH 7	5.3	12

[a] % Degradation = $[1 - A_{517nm}(t)/A_{517nm}(t = 0)]\cdot 100\%$

Table 3. Extent of Eosin-Y Degradation in oxic conditions with and without HQ.

Electrochemical in-situ monitoring of HQ redox conversion in the presence of Eosin-Y were conducted in a three-electrode cell during illumination by the green laser. The carbon working electrode was polarized at a potential of 0.15 V versus standard hydrogen electrode (SHE). This is lower than the formal potential of hydroquinone (HQ)/benzoquinone (BQ) redox couple (0.30 V versus SHE at pH 7). In the presence of only HQ, no current is therefore expected to run through the working electrode | solution interface, because no oxidation or reduction takes place under the applied potential. In contrast, if chemical oxidation of HQ to BQ takes place in the solution, a current will be observed due to electrochemical reduction of BQ at the electrode | solution interface (Figure 7, mechanism D).

Amperometric measurements showed an increase in photocurrent by two orders of magnitude under green light illumination in the presence of Eosin-Y compared to the buffer solution containing only HQ (Table 2). In the absence of hydroquinone either with or without Eosin-Y added, no such current was observed. Moreover, in anoxic conditions the illumination of the solution containing Eosin-Y and HQ did not result in any noticeable current response.

These observations confirm the hypothesis that the photodegradation mechanism of Eosin-Y in oxic conditions is mediated by singlet oxygen and, probably, by secondary reactive oxygen species. An alternative possible mechanism that was suggested in some published report [38,8] involves redox transformation of EY* (Figure 7, mechanism E). However, this is not supported by our data because no redox transformation of HQ, nor the electrochemical reduction of Eosin-Y was observed in anoxic conditions under illumination.

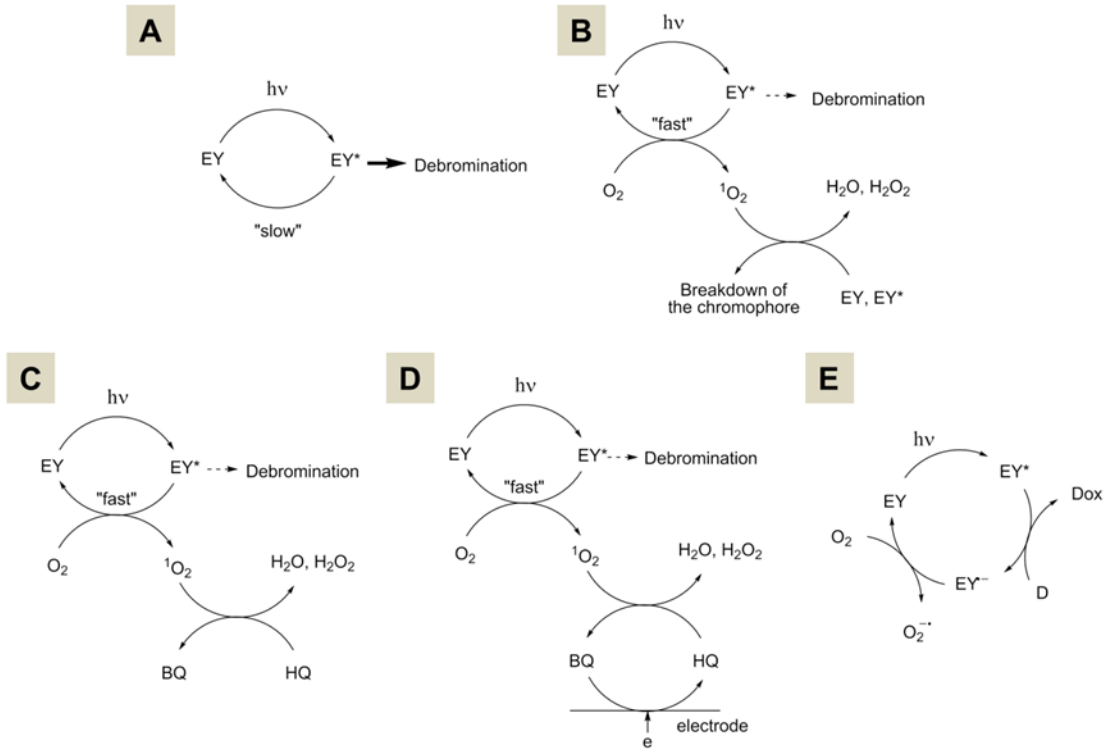

Fig. 7. Schematic representation of the mechanisms of Eosin-Y (EY) discoloration in oxic and anoxic conditions. EY*: photo-excited triplet EY. The mechanisms A and B are supported by our data, while the mechanism E, where D is an electron donor (HQ, EY or electrode) is not supported by our data. Debromination in oxic conditions is suppressed because of decrease in a steady-state concentration of EY in the excited state. The presence of HQ suppresses discoloration of EY in oxic conditions (mechanism C). Mechanism D shows redox cycling of HQ during electrochemical measurements under illumination.

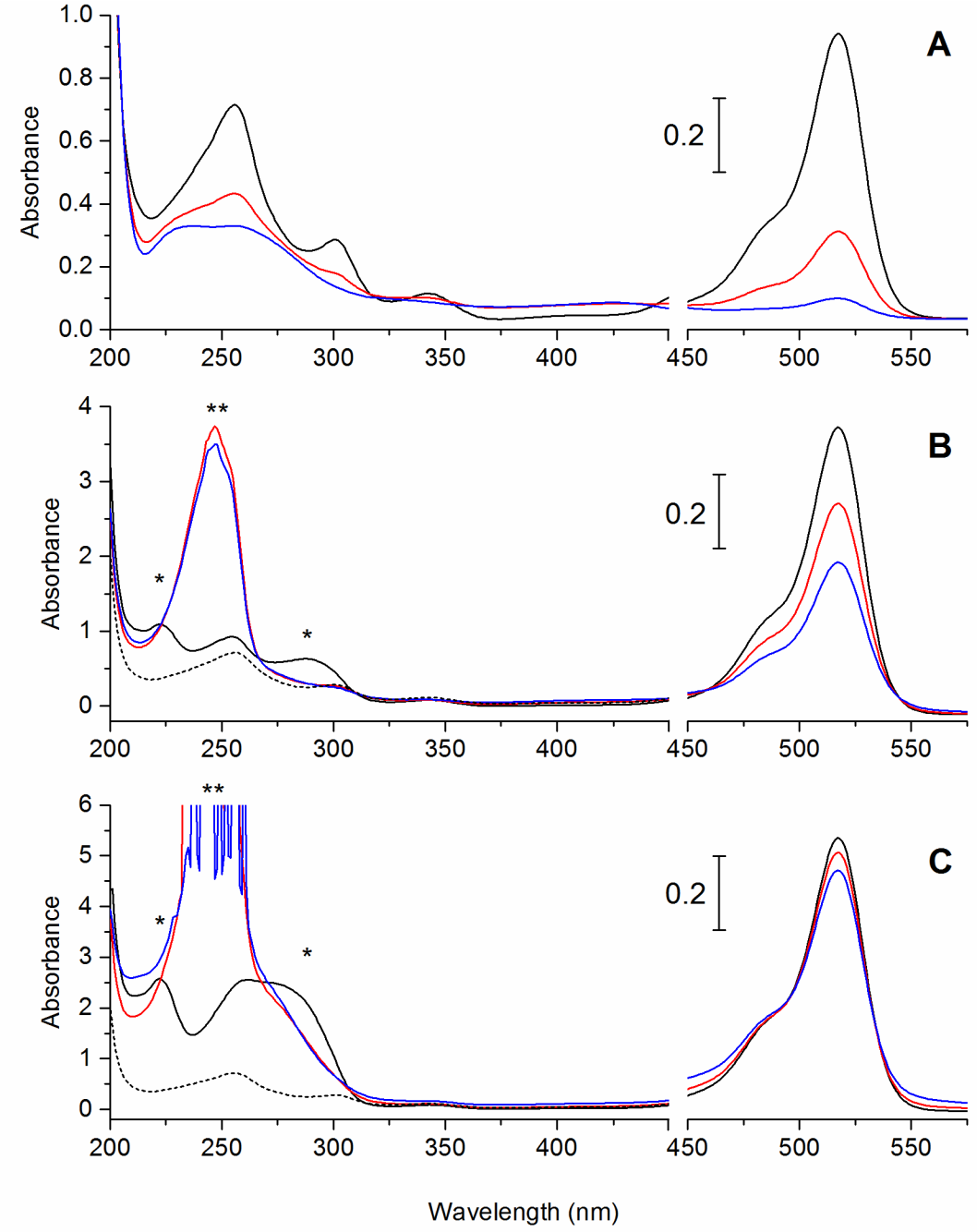

436

437 **Fig. 8.** UV-VIS spectra of photodegradation under green laser: (A) 15 μM Eosin-Y, pH 7 (B) 15

438 μM Eosin-Y + 150 μM HQ, pH 7 and (C) 15 μM Eosin-Y + 450 μM HQ, pH 7. Absorbance bands

439 of HQ (221 and 288 nm) and BQ (245 nm) are indicated by single and double asterisks. The dashed

440 line denotes the spectrum of 15 μM Eosin-Y in absence of HQ.

4. Conclusions

The study of the degradation of Eosin-Y in aqueous solutions clarified the relationship between the rate of degradation, the light wavelength employed and the oxic/anoxic conditions.

The main contribution proposed in this paper is the combination of UV-VIS spectrophotometry, LC-QTOFMS and electrochemistry analyses in order to elucidate the photodegradation pathways of organic pigments.

Spectroscopy and chromatography means allowed highlighting differences in degradation kinetics when different illumination conditions were employed.

It is remarkable that a significant difference in the degradation rate between oxic and anoxic conditions was observed. The dissimilarities in the kinetics have been ascribed to different degradation mechanisms. This result can be explained by the results provided in the LC-QTOFMS analysis of the irradiated samples, where two debromination products were detected. The single debromination product was observed in samples under oxic and anoxic conditions, but the double debromination product was only identified under N_2 atmosphere.

These different pathways are endorsed by the electrochemical experiments carried out in this study. In the presence of oxygen, a fast reaction between photo-excited Eosin-Y and oxygen species takes place, resulting in the breakdown of the molecule and giving rise to the discoloration phenomenon. Under anoxic conditions, the photo-excited Eosin-Y molecules are subject to a slower debromination process. This involves two stages, giving rise to single and double debrominated products. However, this process does not imply complete discoloration since the chromophoric group remains essentially intact. This study shows that the significant stabilization of the degradation/discoloration of Eosin-Y may be realized by the removal of oxygen from the environment.

References

[1] Geldof M, de Keijzer M, van Bommel M, Pilz K, Salvant J, van Keulen H, et al. Van Gogh's geranium lake. In: Vellekoop M, Jansen L, Geldof M, Hendriks H, de Tagle A, editors. Van Gogh's Studio Practice: Mercatorfonds; 2013.

[2] Claro A, Melo MJ, Schäfer S, de Melo JSS, Pina F, van den Berg KJ, et al. The use of microspectrofluorimetry for the characterization of lake pigments. Talanta 2008;74(4):922-9.

[3] Anselmi C, Capitani D, Tintaru A, Doherty B, Sgamellotti A, Miliani C. Beyond the color: A structural insight to eosin-based lakes. Dyes Pigm 2017;140:297-311

[4] Hendriks E, Jansen L, Salvant J, Ravaud E, Eveno M, Menu M, et al. A Comparative Study of Vincent van Gogh's Bedroom Series. Studying Old Master Paintings: Technology and Practice. Natl Gallery Tech Bull. 20th Anniversary Conference Postprints; 2010. p. 237-43.

[5] Burnstock A, Lanfear I, van der Berg K, Carlyle L, Clarke M, Hendriks E, et al. Preprints of the 14th Triennial Meeting of the ICOM Committee for Conservation. The Hague; 2005. p. 459-66.

[6] van Driel BA, Kooyman PJ, van den Berg KJ, Schmidt-Ott A, Dik J. A quick assessment of the photocatalytic activity of TiO2 pigments — From lab to conservation studio!. Microchem J 2016;126:162-71.

[7] Rader Bowers LM, Schmidtke Sobeck SJ. Impact of medium and ambient environment on the photodegradation of carmine in solution and paints. Dyes Pigm 2016;127:18-24.

[8] Majek M, Filace F, von Wangelin AJ. On the mechanism of photocatalytic reactions with eosin Y. Beilstein J Org Chem 2014;10:981-9.

[9] Zheng H, Pan Y, Xiang X. Oxidation of acidic dye Eosin Y by the solar photo-Fenton processes. J Hazard Mater 2007;141(3):457-64.

[10] Korenberg C. The photo-ageing behaviour of selected watercolour paints under anoxic conditions. Br Mus Tech Res Bull 2008;2:49-57.

[11] Townsend JHT, Jacob; Hackney, Stephen; Lerwill, Andrew. The benefits and risks of anoxic display for colorants. Stud Conserv 2008;53:76-81.

[12] Saito M, Minemura C, Nanashima N, Kashiwagi M. Color Fading Behavior of Anthraquinone Dyes Due to Environmental Conditions. Text Res J 1988;58(8):450-4.

[13] Burke J. Personal Communication. Oakland Museum Conservation, Oakland, CA; 1997.

[14] Brott Buss JJ, Cox Crews PC. Influence of nitrogen gas and oxygen scavengers on fading and color change in dyed textiles. Faculty Publications - Textiles, Merchandising and Fashion Design; 2000.

[15] Allen AE, MacMillan DWC. Synergistic Catalysis: A Powerful Synthetic Strategy for New Reaction Development. Chem Sci 2012;3:633-58.

[16] Neumann M, Füldner S, König B, Zeitler K. Metal-Free, Cooperative Asymmetric Organophotoredox Catalysis with Visible Light. Angew Chem Int Ed 2011;50(4):951-4.

[17] Liu Q, Li Y-N, Zhang H-H, Chen B, Tung C-H, Wu L-Z. Reactivity and Mechanistic Insight into Visible-Light-Induced Aerobic Cross-Dehydrogenative Coupling Reaction by Organophotocatalysts. Chem Eur J 2012;18(2):620-7.

[18] Bi Y, Neckers DC. Photochemical reaction of halogenated xanthene dye with diaryliodonium salts. J Photochem Photobiol A 1993;74(2–3):221-30.

[19] Anaf W, Janssens K, De Wael K. Formation of Metallic Mercury During Photodegradation/Photodarkening of α-HgS: Electrochemical Evidence. Angew Chem Int Ed 2013;52(48):12568-71.

510 [20] Anaf W, Trashin S, Schalm O, van Dorp D, Janssens K, De Wael K. Electrochemical
511 photodegradation study of semiconductor pigments: influence of environmental parameters. Anal
512 Chem 2014;86(19):9742-8.
513 [21] Greeneltch NG, Davis AS, Valley NA, Casadio F, Schatz GC, Van Duyne RP, et al. Near-
514 Infrared Surface-Enhanced Raman Spectroscopy (NIR-SERS) for the Identification of Eosin Y:
515 Theoretical Calculations and Evaluation of Two Different Nanoplasmonic Substrates. J Phys Chem
516 A 2012;116(48):11863-9.
517 [22] Claro A, Melo MJ, Seixas de Melo JS, van der Berg KJ, Burnstock A, Montague M, et al.
518 Identification of red colorants in Van Gogh paintings and ancient Andean textiles by
519 microspectrofluorimetry. J Cult Herit 2010;11:27-34.
520 [23] De S, Das S, Girigoswami A. Environmental effects on the aggregation of some xanthene dyes
521 used in lasers. Spectrochim Acta Part A 2005;61(8):1821-33.
522 [24] Batistela VR, Pellosi DS, de Souza FD, da Costa WF, de Oliveira Santin SM, de Souza VR,
523 et al. pKa determinations of xanthene derivates in aqueous solutions by multivariate analysis
524 applied to UV–Vis spectrophotometric data. Spectrochim Acta Part A 2011;79(5):889-97.
525 [25] Johnston-Feller R, Feller RL, Bailie CW, Curran M. The Kinetics of Fading: Opaque Paint
526 Films Pigmented with Alizarin Lake and Titanium Dioxide. J Am Inst Conserv 1984;23(2):114-
527 29.
528 [26] Espensor JH. Chemical Kinetics and Reactions Mechanism. 2nd Edition ed. New York:
529 McGraw Hill; 1987.
530 [27] Feller RL, Johnston-Feller RM, Bailie C. Determination of the Specific Rate Constant for the
531 Loss of a Yellow Intermediate during the Fading of Alizarin Lake. J Am Inst Conserv
532 1986;25(2):65-72.

[28] Arbeloa EM, Previtali CM, Bertolotti SG. Photochemical study of Eosin-Y with PAMAM dendrimers in aqueous solution. J Lumin 2016;180:369-75.

[29] Kimura K, Miwa T, Imamura M. Photochemical debromination of eosin in basic methanolic solution. Chem Commun (London) 1968;24:1619-21.

[30] Kimura K, Miwa T, Imamura M. The Radiolysis and Photolysis of Methanolic Solutions of Eosin. II. The Photo-Debromination of Eosin in an Alkaline Solution. Bull Chem Soc Jpn 1970;43(5):1337-42.

[31] Peters AT, Tenny BA. Brominated Diamino Dihydroxyanthraquinones. Blue Dyes for Synthetic-polymer Fibres. J Soc Dyers Colour 1977;93(10):378-86.

[32] Koren ZC. Chromatographic and colorimetric characterizations of brominated indigoid dyeings. Dyes Pigm 2012;95(3):491-501.

[33] Hari DP, Konig B. Synthetic applications of eosin Y in photoredox catalysis. Chem Commun 2014;50(51):6688-99.

[34] Redmond RW, Gamlin JN. A Compilation of Singlet Oxygen Yields from Biologically Relevant Molecules. Photochem Photobiol 1999;70(4):391-475.

[35] Amat-Guerri F, López-González MMC, Martínez-Utrilla R, Sastre R. Singlet oxygen photogeneration by ionized and un-ionized derivatives of Rose Bengal and Eosin Y in diluted solutions. J Photochem Photobiol A 1990;53(2):199-210.

[36] Gandin E, Lion Y, Van de Vorst A. Quantum Yield of Singlet Oxygen Production by Xanthene Derivatives. Photochem Photobiol 1983;37(3):271-8.

[37] García NA. New trends in photobiology. J Photochem Photobiol B 1994;22(3):185-96.

[38] Hari DP, König B. Eosin Y Catalyzed Visible Light Oxidative C–C and C–P bond Formation. Org Lett 2011;13(15):3852-5.

Supplementary Information

Photodegradation mechanisms and kinetics of Eosin-Y in oxic and anoxic conditions

Alba Alvarez-Martin[a,*], Stanislav Trashin[a], Matthias Cuykx[b], Adrian Covaci[b], Karolien De Wael[a], Koen Janssens[a]

[a] AXES, Department of Chemistry, University of Antwerp, Groenenborgerlaan 171, 2020 Antwerp, Belgium

[b] Toxicological Center, University of Antwerp, Universiteitsplein 1, 2610 Wilrijk, Belgium

[*]Corresponding author E-mail address: alba.alvarez@usal.es (Alba Alvarez-Martin)

Table SI.1. Experimental molar absorptivity coefficients of Eosin-Y.

λ_{max} (nm)	ε (M^{-1} cm^{-1})
517	1.1×10^5
341	0.8×10^4
301	0.2×10^5
225	0.3×10^5

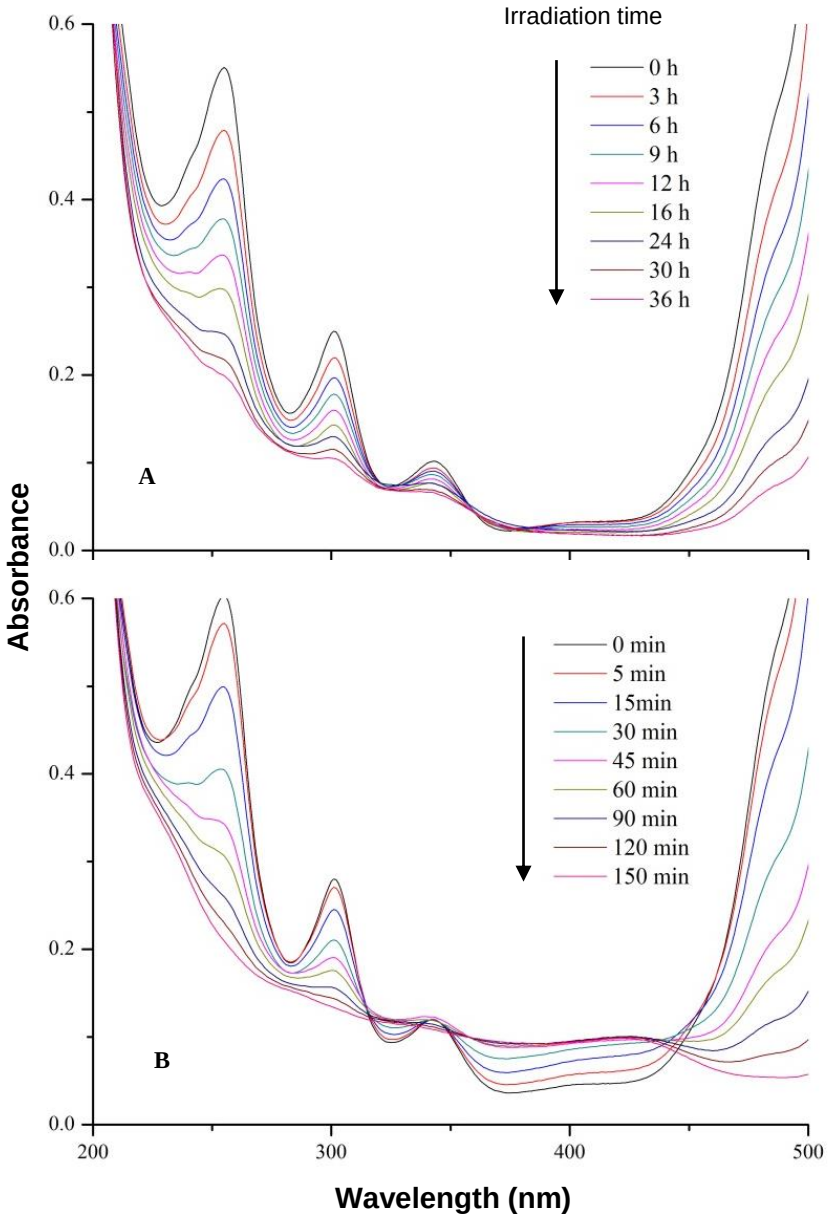

574

575 **Fig. SI.1.** UV-VIS spectra of photodegradation of Eosin-Y under oxic condition irradiated with:

576 (A) blue laser (405 nm) and (B) green laser (532 nm).

577

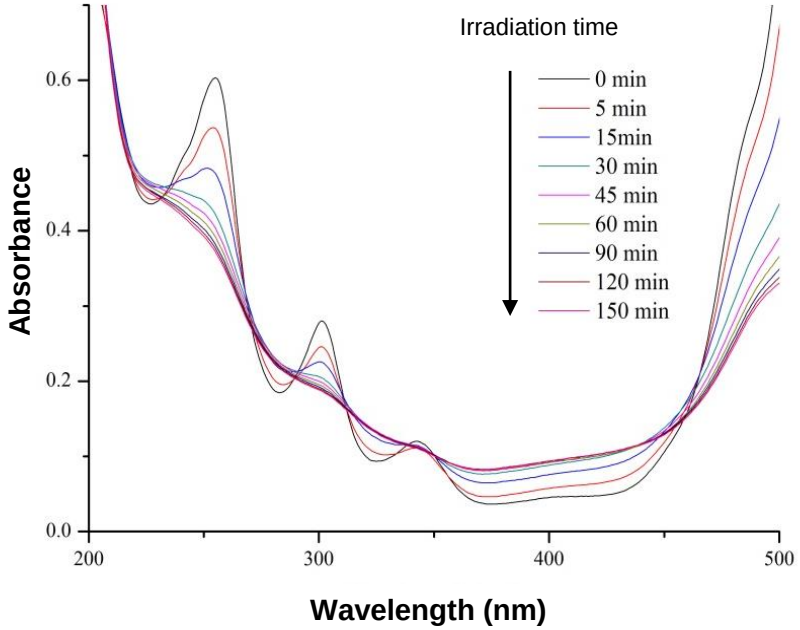

578

579 **Fig. SI.2.** UV-VIS spectra of photodegradation of Eosin-Y under anoxic condition irradiated with

580 green laser (532 nm).

581

582

583

584

585

586

587

588

589

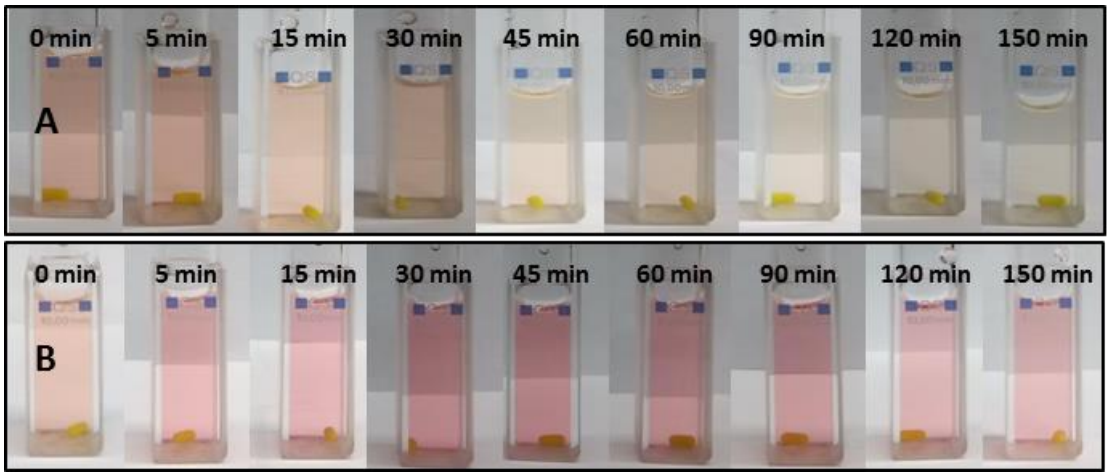

Fig. SI.3. Photographs of Eosin-Y after irradiation with green laser at different time intervals under oxic (A) and anoxic (B) conditions.

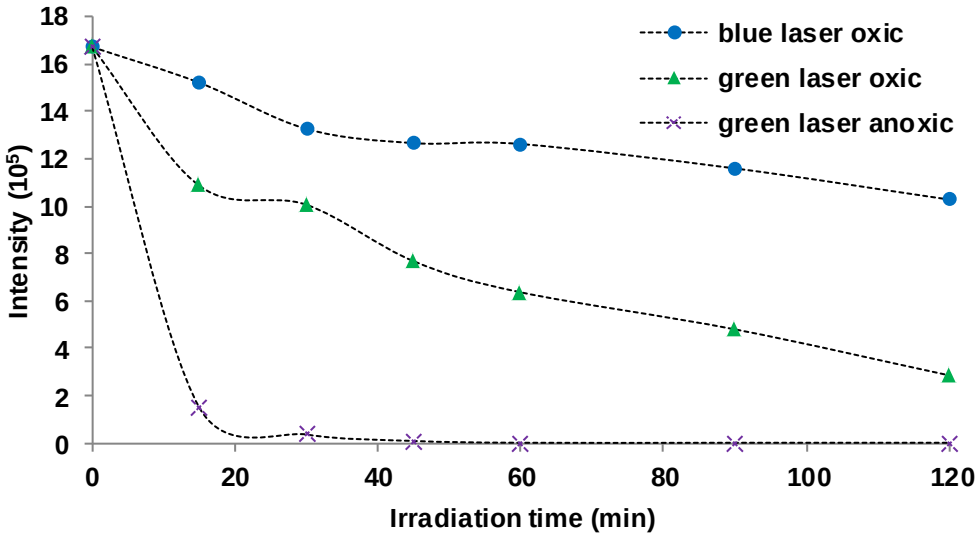

Fig. SI4. Qualitative estimation of Eosin-Y (m/z = 646.69) degradation by LC-QTOFMS.

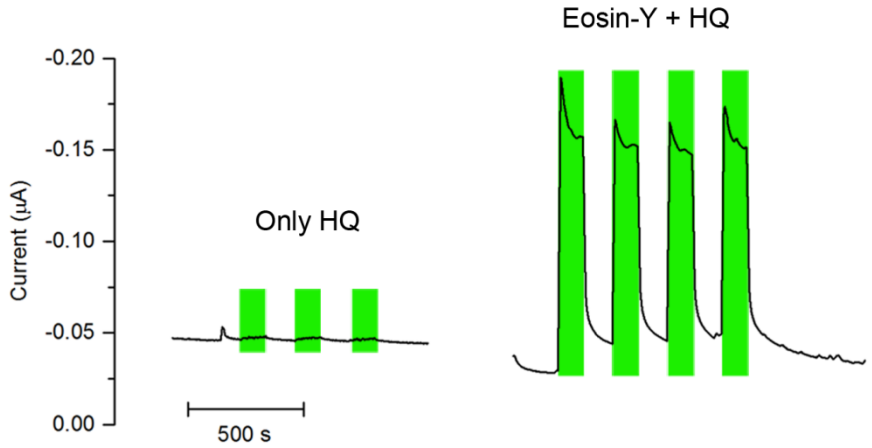

Fig. SI.5. Amperometry in the presence and absence of Eosin-Y in the air saturated buffer (oxic conditions) containing 10 µM HQ.

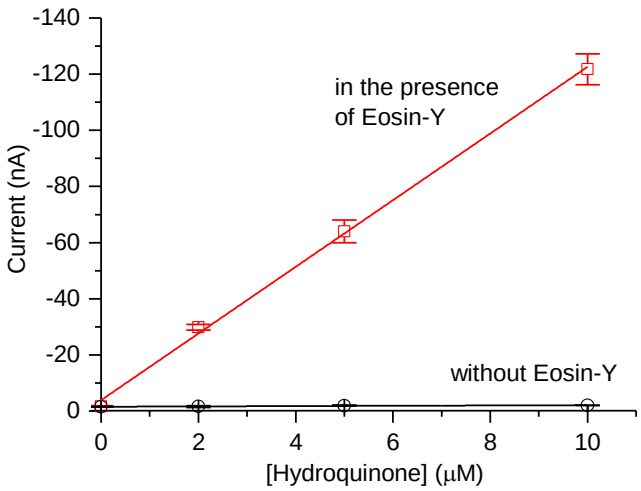

611

612 **Fig. SI.6.** Photocurrent measured under illumination with the green laser in the presence of

613 hydroquinone of different concentrations (HQ) and with or without 10 μM Eosin-Y in solution.

614

615

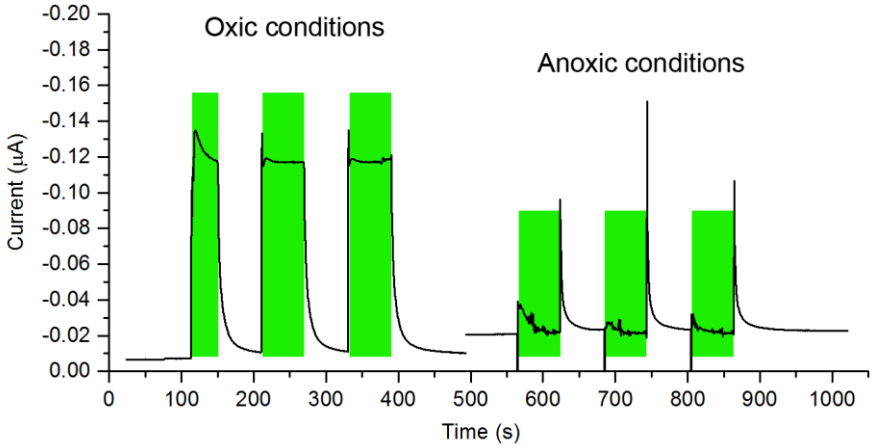

616

617 **Fig. SI.7.** Amperometry in the presence of 10 μM HQ and 10 μM Eosin-Y in air saturated buffer

618 (oxic conditions and) and under N_2 atmosphere (anoxic conditions).

619

620

Figure Captions

Fig.1. Chemical structure of Eosin-Y. Lactone form (A), Quinoid form (B) and Dianionic form (C).

Fig.2. UV-VIS spectra of photodegradation of Eosin-Y under oxic conditions irradiated with (A) the 405 nm (blue) and (B) the 532 nm (green) laser.

Fig. 3. First-order linear plot of $\ln[A_{517nm}(t=0)/A_{517nm}(t)]$ vs the irradiation time t under irradiation by three light sources (532 nm, 405 nm and 300-350 nm).

Fig. 4. UV-VIS spectra of Eosin-Y during photodegradation under anoxic conditions, irradiated with a 532 nm laser.

Fig. 5. Pseudo first-order linear plot of $\ln[A_{517nm}(t=0)/A_{517nm}(t)]$ vs irradiation time *t* under 532 nm (green) laser irradiation and anoxic conditions.

Fig. 6. Formation and decay of transformation products (A) $C_{20}H_9O_5Br_3$ (m/z = 566.7886) and (B) $C_{20}H_{10}O_5Br_2$ (m/z = 488.8759).

Fig. 7. Schematic representation of the mechanisms of Eosin-Y (EY) discoloration in oxic and anoxic conditions. EY*: photo-excited triplet EY. The mechanisms A and B are supported by our data, while the mechanism E, where D is an electron donor (HQ, EY or electrode) is not supported by our data. Debromination in oxic conditions is suppressed because of decrease in a steady-state concentration of EY in the excited state. The presence of HQ suppresses discoloration of EY in oxic conditions (mechanism C). Mechanism D shows redox cycling of HQ during electrochemical measurements under illumination.

Fig. 8. UV-VIS spectra of photodegradation under green laser: (A) 15 μM Eosin-Y, pH 7 (B) 15 μM Eosin-Y + 150 μM HQ, pH 7 and (C) 15 μM Eosin-Y + 450 μM HQ, pH 7. Absorbance bands

643 of HQ (221 and 288 nm) and BQ (245 nm) are indicated by single and double asterisks. The dashed

644 line denotes the spectrum of 15 μM Eosin-Y in absence of HQ.